Item-specific memory reactivation supports overnight memory consolidation

Jing Liu[1,2], Tao Xia[2,3], Danni Chen[2,3], Ziqing Yao[2,3], Minrui Zhu[2,3],

James Antony[4], Tatia M.C. Lee[2,5*], Xiaoqing Hu[2,3,6*]

1. Department of Applied Social Sciences, The Hong Kong Polytechnic University, Hong Kong SAR, China

2. The State Key Laboratory of Brain and Cognitive Sciences, The University of Hong Kong, Hong Kong SAR, China

3. Department of Psychology, The University of Hong Kong, Hong Kong SAR, China

4. Department of Psychology & Child Development, California Polytechnic State University, California, USA

5. Laboratory of Neuropsychology and Human Neuroscience, Department of Psychology, The University of Hong Kong, Hong Kong SAR, China

6. HKU-Shenzhen Institute of Research and Innovation, Shenzhen 518057, China

* Correspondence should be sent to:

T.M.C. L., tmclee@hku.hk; X. H., xiaoqinghu@hku.hk;

The authors declare no conflict of interests

Abstract

Understanding how individual memory traces are reactivated during sleep is instrumental to the theorizing of memory consolidation, a process during which newly acquired information becomes stabilized and long-lasting. Via targeted memory reactivation (TMR), a technique that unobtrusively delivers learning-related memory cues to sleeping participants, we examined the reactivation of individual memories during slow-wave sleep and how canonical neural oscillations support item-specific memory reactivation. Furthermore, we investigated how pre-sleep testing, which presumably induces fast consolidation before sleep, would modulate sleep-mediated memory reactivation. Applying multivariate representational similarity analysis (RSA) to the cue-elicited electroencephalogram (EEG), we identified significant item-specific representations in two post-cue time windows (620-1350 ms and 2270-3190 ms) for post-sleep remembered items, with only the later item-specific representations contributing to memory consolidation. Untested items (i.e., items that were not tested pre-sleep), but not tested items, elicited higher spindles that predicted stronger item-specific representations and post-sleep memories. Notably, for untested items, the strengths of memory reactivation and spindles were temporally coupled to the up-state of the slow oscillation activity. Together, our results unveiled how item-specific memory reactivation and its link with neural oscillations during sleep contributed to memory consolidation. This knowledge will benefit future research aiming to perturb specific memory episodes during sleep.

Keywords: memory consolidation, targeted memory reactivation, representational similarity analysis, slow-wave sleep, spindle, slow oscillation up-state

Introduction

Newly acquired experiences undergo consolidation before they can become long-lasting memories (McGaugh, 2000). Mounting evidence from various techniques (e.g., single-unit recordings, fMRI, EEG) and species suggests that sleep consolidates memory via repeated, covert reactivation of memories during post-learning non-rapid eye movement (NREM) sleep (Born & Wilhelm, 2012; Klinzing et al., 2019; Schönauer et al., 2017; Schreiner et al., 2021; Sterpenich et al., 2021; Wilson & McNaughton, 1994; Zhang et al., 2018). Intriguingly, memory reactivation can be maneuvered by unobtrusively re-presenting sensory cues associated with wakeful learning during sleep, a paradigm known as targeted memory reactivation (TMR) (Bendor & Wilson, 2012; Hu et al., 2020; Rasch et al., 2007; Rudoy et al., 2009). Compared with research that examines spontaneous memory reactivation during sleep, TMR allows researchers to manipulate when and which specific memories become reactivated via re-playing memory cues. Given the challenges in identifying the neuronal ensembles subserving cue-elicited memory reactivation in humans, memory reactivation during TMR session is usually inferred based on memory differences between cued versus uncued items in post-sleep tests, i.e., TMR benefits. Despite established TMR benefits on behavior (Hu et al., 2020), exactly how specific memories are reactivated during sleep is far from clear.

Recently, advances have been made with the multivariate neural decoding methods: TMR cue-elicited neural activity contained task-related or category-level memory representations that are associated with subsequent TMR benefits (Belal et al., 2018; Cairney et al., 2018; Shanahan et al., 2018; Wang et al., 2019). In addition, pre-sleep memory content may re-occur rhythmically following TMR cues (Lewis & Bendor, 2019; Schreiner et al., 2018), with memory reactivation tightly linked with neural oscillations during sleep. Specifically, research shows that enhanced post-cue spindle-related sigma power positively predicted TMR benefits (Antony et al., 2018; Fuentemilla et al., 2013), while reduction of sigma power was associated with weakened TMR benefits (Schreiner et al., 2015). Relatedly, TMR benefits are abolished when cueing occurs during the spindle refractory period, i.e., a 3-6 s period following a spindle when a spindle is less likely to occur (Antony et al., 2018). The intriguing idea is that an intact, undisrupted spindle refractory period could be instrumental in continuing to process the reactivated memory, which

could contribute to memory consolidation (Antony et al., 2019; Lewis & Bendor, 2019; Schönauer, 2018).

Notwithstanding this promising progress, fundamental questions remain. Foremost, although the behavioral evidence supporting that TMR selectively benefits cued items, the neural evidence for memory reactivation of individual items, beyond categorical information, remains scarce. Second, how the reactivation of item-specific representations dynamically changes over time remains unclear. For example, is reactivation evident during the entire post-cue period, or does it re-occur rhythmically (Schreiner et al., 2018)? If reactivation occurs in segregated time windows, will the item-specific reactivation in different time windows bear distinct functional significance? Lastly, how are the canonical neural oscillations during sleep, such as spindles and slow oscillations, among other EEG activities, subserving item-specific memory reactivation and, ultimately, leading to memory consolidation?

Another important factor that may modulate the TMR benefits is pre-sleep testing. Pre-sleep testing could enhance memory presumably via fast consolidation processes (Antony et al., 2017; Roediger & Butler, 2011) and thereby influence TMR benefits during the following sleep-mediated consolidation. Indeed, research shows that pre-sleep memory strength modulated both sleep's and TMR's impacts on memory consolidation, although with mixed findings (Cairney et al., 2016; Creery et al., 2015; Denis et al., 2021; Schapiro et al., 2018). One recent study also found that TMR was only effective in modulating memory performance for pre-sleep untested items, but not for pre-sleep tested items (Joensen et al., 2022). However, it remains unclear how pre-sleep testing would modulate the item-specific memory reactivation and the associated neural oscillations during sleep. Bridging this gap will contribute to our understanding of the interaction between wakeful, retrieval-based consolidation and sleep-mediated reactivation-based consolidation.

Representational similarity analysis (RSA) combing with EEG recordings provides a powerful tool to extract item-specific representation and its dynamics across time (Feng et al., 2019; Liu et al., 2021; Lu et al., 2015). Here, we applied RSA to TMR cue-elicited EEG activities during slow-wave sleep. We identified significant item-specific representations in two temporally segregated time windows following TMR cues for post-sleep remembered items. While item-specific representations in the early time window were mainly driven by the processing of

external sensory cues, item-specific representations in the late time window reflected cue-triggered memory reactivation, which predicted long-term memory. Notably, pre-sleep testing significantly modulated the item-specific memory reactivation and its link with neural oscillations during sleep: only pre-sleep untested items were associated with increased spindles that supported item-specific representations in the late time window and peaked at slow oscillation up-phases.

Results

Behavioral results

Thirty-three participants (25 females, mean ± SD age, 21.91 ± 2.65 years) were included in the analyses. Participants learned 96 word-picture (cue-target) pairs during the encoding phase. Specifically, in each trial, a word-picture pair was presented for 2 s, during which participants heard the spoken word from a loudspeaker while viewing the picture presented on the screen. This was followed by a 3-s maintenance period, during which only the spoken cue word was played, and participants were asked to mentally maintain the visual image of the picture that was associated with the cue word. Each word-picture pair was repeated three times during the encoding phase. After a distractor (math) task, participants completed a pre-sleep cued recall test, wherein half (48) of the learning pairs were tested (i.e., tested items) while the other half (48) were untested (i.e., untested items). TMR cues consisted of 24 spoken words from each of the tested and untested items respectively, resulting in a total of 48 TMR cues. For tested items, cued and uncued items were matched for pre-sleep cued-recall performance. For untested items, cues were pseudo-randomly selected (see Methods). In addition to these 48 TMR cues, four novel spoken words that were not paired with any learning content and served as control cues were played the same number of times as TMR cues during sleep. On the following morning, memory was tested for all 96 learned pairs (see Fig. 1).

We first examined how pre-sleep testing affected TMR benefits by conducting a 2 (cued vs. uncued) by 2 (tested vs. untested) repeated measures ANOVA on post-sleep memory recall performance. Results revealed neither a significant interaction effect ($F(1,32) = 0.23$, $p = 0.637$) nor a significant main effect of TMR (cued vs. uncued, $F(1,32) = 0.16$, $p = 0.690$) (see Fig. S1). The same ANOVA on the post-sleep memory recognition performance also revealed neither a

significant TMR by pre-sleep testing interaction effect nor a main effect of TMR (all *ps* > 0.789, see Fig. S1). Despite the non-significant TMR benefits at the group level, we observed substantial individual differences (see Fig. S1) and aimed to further examine the relationship between cue-elicited neural activity and TMR benefits across participants. We, therefore, used the cued-recall performance, a more sensitive behavioral index than recognition for TMR effects (see Hu et al., 2020), in the following analyses.

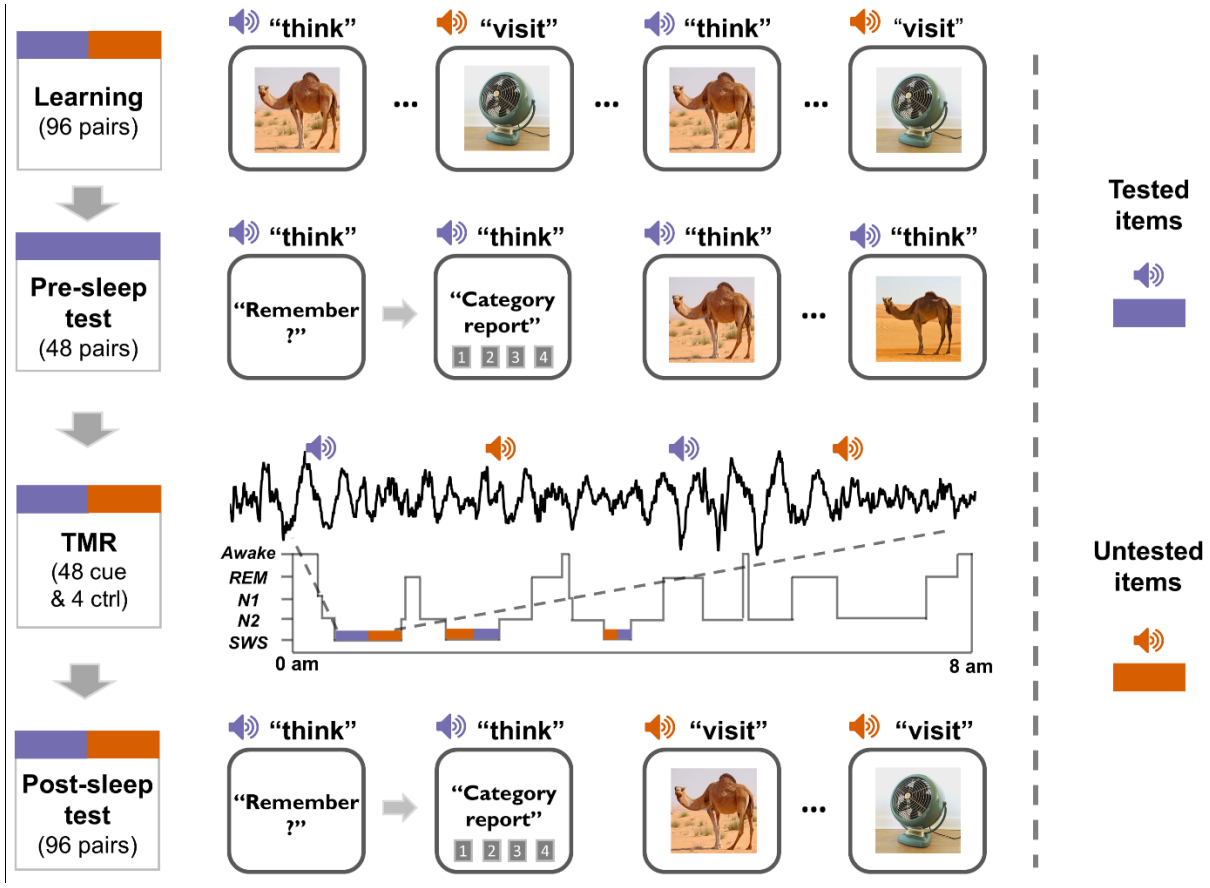

Fig 1. Experimental design. The experiment included four phases, including learning, a pre-sleep test (cued recall and recognition), targeted memory reactivation (TMR) during SWS, and a post-sleep test. Participants learned 96 word-picture pairs during learning, with each pair being repeated three times. Half the pairs were tested during the pre-sleep test (i.e., tested items, blue rectangle) in both the cued-recall task and the recognition task. The remaining half pairs were untested items (orange rectangle). Auditory cues from half of the tested items and half of the untested items, intermixed with four control cues, were played during the SWS stage of the overnight sleep. Cues were randomly presented with an inter-stimuli interval of 5 ± 0.2 s. Memory for all 96 pairs was tested again during the post-sleep test in both the cued-recall task and the recognition task the next morning.

TMR-elicited EEG activity predicted TMR benefits for untested items

Previous studies showed that external auditory stimulation during NREM sleep elicited increased theta (~4-7 Hz), alpha (~8-12 Hz), and sigma (~11-16 Hz) bands activity (Cairney et al., 2018; Wislowska et al., 2022). To ensure that the auditory memory cues were processed during sleep, we contrasted the spectral power in a 5-s time window post-cue onset versus the pre-cue baseline ([-1, -0.5 s] relative to cue onset). In line with previous studies, auditory cues across all tested and untested items significantly enhanced EEG power in a broad range of 1-40 Hz within the first 2780 ms following the cue onset ($p_{corr} < 0.001$, see Fig. 2A), with two prominent frequency ranges: a low, 1-10 Hz frequency range and an extended 11-19 Hz sigma band. Following this early cluster, we also observed a significant reduction of sigma power in a late cluster (2100-3790 ms, $p_{corr} = 0.002$), which potentially reflected the spindle refractoriness (Antony et al., 2018).

We next performed the robust linear regression model analysis to better ask how TMR-elicited EEG power change affected behavioral outcomes while minimizing the influence of potential statistical outliers. The results revealed that TMR-elicited EEG power in the early cluster (within the first 2780 ms) positively predicted TMR benefits across participants (adjusted $R^2 = 0.155$, $p = 0.015$). The same analysis showed that both the low-frequency (1-10 Hz) and the sigma (11-19 Hz) power band in the early cluster significantly predicted TMR benefits (adjusted $R^2 > 0.14$, all ps < 0.023, Fig. 2B-C). More specifically, delta (1-3 Hz), theta (4-7 Hz), and alpha (8-12 Hz) band power significantly predicted TMR benefits respectively (all ps < 0.013). The same robust linear regression analysis on the sigma band power decrease in the late negative cluster (i.e., 2100-3790 ms), however, showed a non-significant effect (adjusted $R^2 = 0.01$, $p = 0.268$).

We further examined how pre-sleep testing modulated the relationship between cue-elicited EEG spectral power and the TMR benefits by separating tested and untested items. We found that tested and untested items showed enhanced cue-elicited EEG power changes in the first ~2 s (1-40 Hz, $p\text{s}_{corr} < 0.001$), which was followed by a significant sigma power decrease ($p\text{s}_{corr} < 0.018$) (Fig. S2A-B), while there were no significant differences between tested and untested items ($p\text{s}_{corr} > 0.335$, Fig. S2C). Nevertheless, pre-sleep testing remarkably modulated the relationship between cue-elicited EEG power change and TMR benefits. For tested items, neither the low-frequency nor the sigma band EEG power within the first 2360 ms (Fig. S2A) predicted TMR

benefits (adjusted $R^2 < 0$, *p*s > 0.465, Fig. 2D-E). In contrast, for untested items, both the low-frequency power (1-10 Hz) and sigma power within the first 2700 ms (Fig. S2B) positively predicted TMR benefits (adjusted $R^2 > 0.19$, *p*s < 0.006) (Fig. 2D-E), and the prediction effects were significantly higher than the tested items (*p*s < 0.003). Together, these results indicated that greater cue-elicited low-frequency (1-10 Hz) and sigma power (11-19 Hz) within the first ~2 s predicted better post-sleep memories for untested items but not tested items.

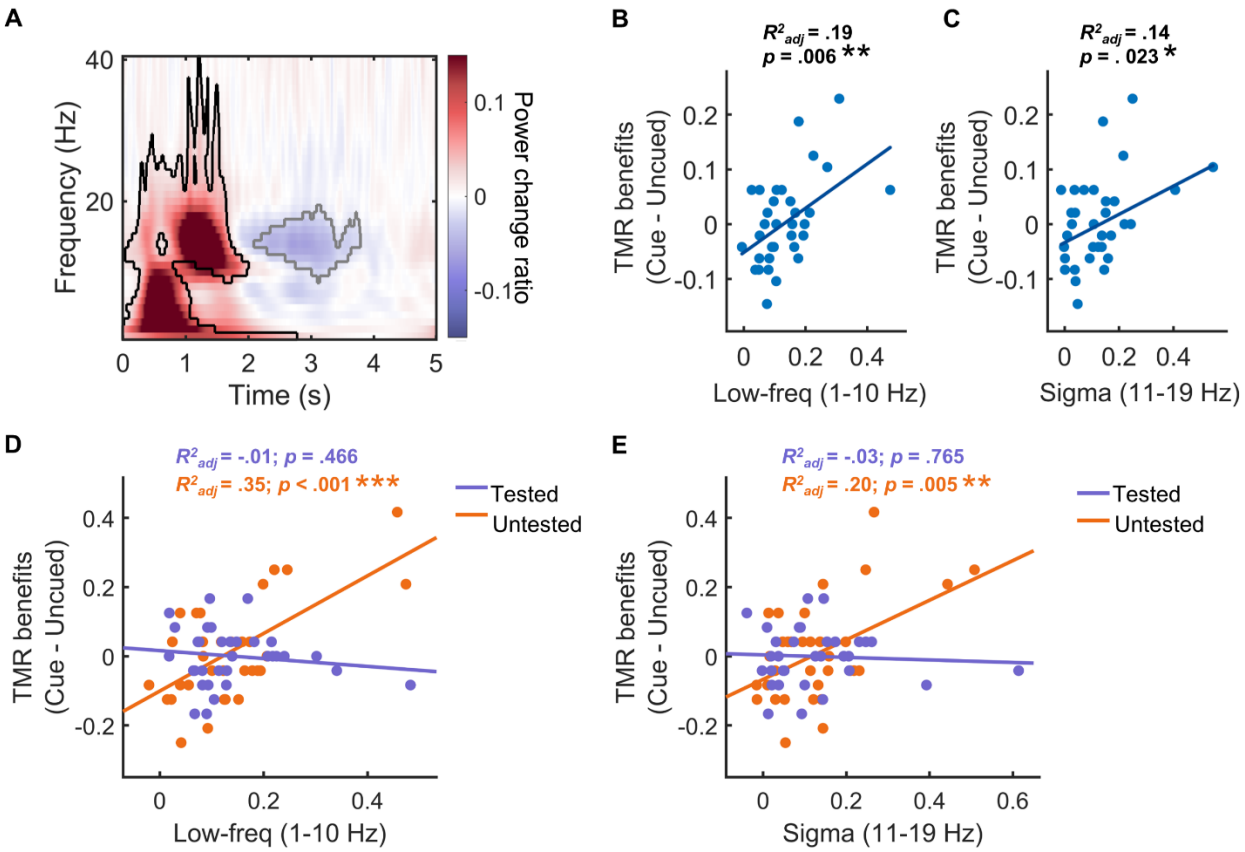

Fig 2. TMR cue-elicited EEG spectral power change in the early cluster (i.e., approximately first 2 s post cue onset) and its link with the post-sleep TMR benefits. (A) Compared to the pre-cue baseline (i.e., 0.5-1 s pre-cue onset), TMR cues across all tested and untested items enhanced EEG spectral power averaged across all electrodes within the first 2780 ms (early cluster, circled by the black line), while decreasing sigma power between 2100-3790 ms (late cluster, circled by the grey line) post-cue onset. **(B-C)** Spectral power changes in the low-frequency range (1-10 Hz) and extended sigma band (11-19 Hz) of the early cluster positively predicted the post-sleep TMR benefits (i.e., memory performance differences between cued and uncued items) across tested and untested items. TMR cue-elicited EEG power change in the low-frequency range (i.e., 1-10 Hz) **(D)** and in the extended sigma band (i.e., 11-19 Hz) of the early cluster **(E)** predicted the post-sleep TMR benefits for untested but not for tested items. *P*-values

indicate the significance of robust linear regression that has been employed to minimize the potential influence of statistical outliers. *: $p < 0.05$; **: $p < 0.01$; ***: $p < 0.001$.

Item-specific representations of cues and their associated memory were reactivated sequentially for subsequently remembered items

TMR promotes memory consolidation via reactivating pre-sleep learning content during subsequent NREM sleep (Wang et al., 2019). The cue-elicited neural activity contains decodable, category-level memory representations (Cairney et al., 2018; Shanahan et al., 2018). Moreover, TMR cues may reinstate item-specific patterns that were associated with pre-sleep wakeful retrieval (Schreiner et al., 2018). However, to the best of our knowledge, no study has examined whether cue-elicited neural activity contains item-specific memory representations during sleep and how such item-specific representations contribute to memory consolidation.

To extract item-specific representations, we performed representational similarity analysis (RSA) between trials of the same cues (within-item [WI] similarity) as well as between trials of different cues (between-item [BI] similarity) (Fig. 3A). Both the WI similarity and BI similarity were calculated between trials from two different TMR blocks to control for the temporal proximity effect (see Methods). The representational similarity was computed by correlating the cue-elicited raw EEG pattern (bandpass filtered between 0.5-40 Hz) across all the channels within consecutive overlapping time windows of 500 ms, with a 10 ms sliding step, during a 5-s time window following the cue onset. Item-specific representations were indicated by significantly greater WI similarity than BI similarity. We first examined whether we could identify item-specific representations across all memory cues and found a significant cluster showing greater WI than BI similarity during 570-1130 ms after cue onset ($p_{corr} = 0.013$, Fig. 3B). Moreover, the pre-sleep testing (tested vs. untested) by item-specificity (WI vs. BI) repeated measures ANOVA did not find any significant interaction clusters ($p_{corr} > 0.097$, see Fig. S3). Therefore, re-playing memory cues during SWS elicited item-specific representations for both tested and untested items.

We next examined our key question: how do cue-elicited item-specific representations impact memory retention? Using the subsequent-memory approach (Paller & Wagner, 2002), we grouped items into subsequently remembered and forgotten items based on post-sleep memory

recall accuracy. We found that subsequently remembered items were associated with significant item-specific representations in two clusters: an early cluster from 620-1350 ms ($p_{corr} = 0.005$) and a late cluster from 2270-3190 ms post cue onset ($p_{corr} = 0.004$, Fig. 3C, see Fig. S4 for the scalp distributions). In contrast, no significant clusters were found for subsequently forgotten items ($p_{corr} > 0.275$). Noteworthy, the item-specific representations were above and beyond category-level representations, given that the WI similarity was greater than the BI similarity when the BI items were drawn from within-category trial pairs (i.e., within-category similarity, WC, see Fig. S5). Thus, TMR cues reactivated item-specific rather than category-level representations during sleep. A 2 (item-specificity: WI vs. BI) x 2 (subsequent memory: remember versus forget) repeated measures ANOVA revealed a significant interaction cluster during 2440-2960 ms, $p_{corr} = 0.022$, (Fig. 3C-D), which highly overlapped with the late item-specific cluster for remembered items (i.e., 2270-3190 ms, Fig. 3C). Post-hoc analyses showed that, in this 2440-2960 ms interaction cluster, subsequently remembered items showed significantly higher WI similarity than BI for remembered items ($t(32) = 3.02$, $p_{FWER} = 0.01$, Fig. 3D, *p*-values were corrected by controlling family-wise error rate, FWER), while no significant effect was found for forgotten items ($t(32) = -1.46$, $p_{FWER} = 0.310$). Thus, stronger item-specific representations during TMR cueing led to better post-sleep memories. Furthermore, an item-specificity (WI vs. BI) by pre-sleep testing (tested vs. untested) repeated measures ANOVA for remembered items did not yield any significant interaction clusters ($p_{corr} > 0.092$), suggesting that item-specific representations led to subsequent remembering for both tested and untested items.

Notably, the fact that the subsequent memory effect only emerged in the late cluster suggested that the item-specific representations in the early and the late time windows may have distinct mechanisms and functional significance. To test this possibility, we conducted a linear mixed-effect model analysis to examine how item-specific representations in the early cluster predicted representations in the late cluster across all memory items and across all participants. The results revealed that the item-specific representations in the early cluster did not predict the item-specific representations in the late cluster ($\beta = 0.03$, $t(1582) = 1.344$, $p = 0.179$), suggesting that item-specific representations in the early and late clusters may contain distinct information.

We further proposed that item-specific representations in the early and late clusters reflected the processing of individual cue words and the reactivation of specific memories, respectively. If this

staged processing hypothesis was true, then control cues, i.e., auditory words that were never paired with any memory and should not reactivate any memory during TMR, would elicit item-specific representations only in the early but not in the late cluster. Consistent with our hypothesis, we found that for control cues, the WI similarity was marginally greater than the BI similarity in the early cluster ($t(32) = 1.89$, $p = 0.068$, Fig. 3E) but not in the late cluster ($t(32) = -1.27$, $p = 0.214$, Fig. 3F). Confirming our hypothesis that only the late cluster would contribute to memory consolidation, we found that subsequently remembered items elicited significantly greater item-specific representations than control cues in the late cluster ($t(32) = 2.89$, $p = 0.007$) but not in the early cluster ($t(32) = -0.31$, $p = 0.762$) (Fig. 3E-F). No significant differences were found between the item-specific representations of subsequently forgotten and control cues in either the early or late clusters (all ps > 0.178). Thus, we provided evidence that item-specific representations were temporally segregated during TMR cueing: while the early cluster (620-1350 ms) primarily reflected sensory-driven representations of individual memory cues, the late cluster (2270-3190 ms) exhibited memory-driven representations, with stronger item-specific representations in the late cluster contributing to long-term memories.

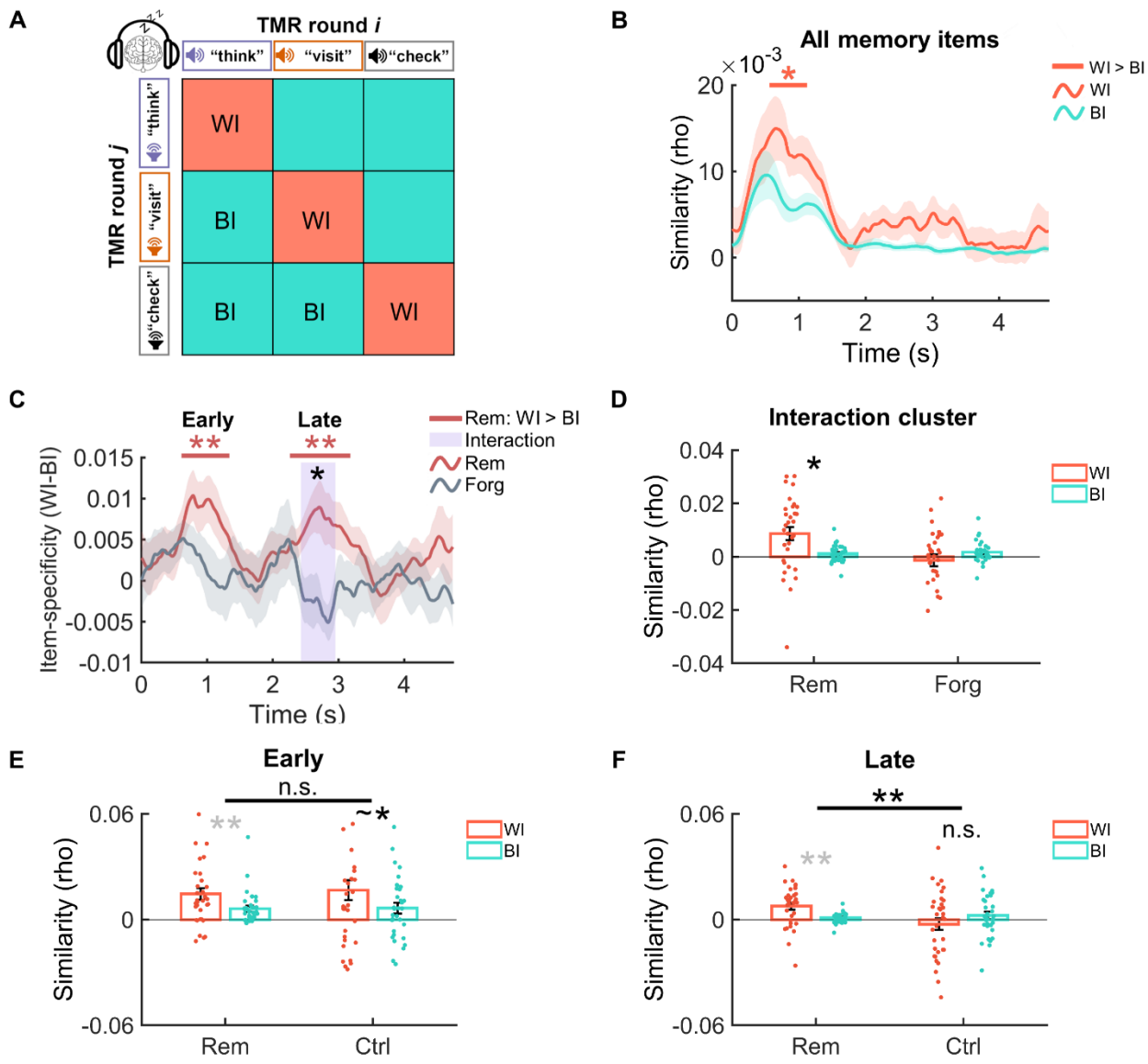

Fig 3. Item-specific representations following TMR cues during slow-wave sleep. (A) Representational similarity analysis across different TMR blocks. EEG activities (0.5-40 Hz) were extracted from all electrodes and were then correlated between TMR cueing trials with the same auditory cues (within-item similarity, WI) as well as between trials with different auditory cues (between-item similarity, BI). Item-specific representations were examined by contrasting the WI similarity versus BI similarity. **(B)** Item-specific representations across all memory items were significant in the time window 570-1130 ms after cue onset, regardless of subsequent memory performance. **(C)** Item-specific representations for all subsequently remembered and forgotten items. For the subsequently remembered items, two significant clusters showed greater WI similarity than BI similarity: an early cluster (620-1350 ms) and a late cluster (2270-3190 ms), indicated by red horizontal lines. No significant clusters were found for forgotten items. There was an additional cluster (2440-2960 ms) showing a significant interaction effect between item-specificity and subsequent memory effect, indicated by the shaded rectangle. **(D)** Post-hoc analyses of the interaction cluster (the shaded rectangle in C) found significant WI > BI

similarities for remembered items, while no differences between WI and BI similarity for forgotten items. **(E)** Control cues showed marginally significant item-specific representations in the early cluster identified in (C), and there was no significant interaction between item-specificity and item type (remembered versus control cues). **(F)** Control cues showed no significant item-specificity in the late cluster identified in (C). The interaction effect between item-specificity and item type was significant, with greater item-specific representations for remembered items than control cues.. *: $p < 0.05$; **: $p < 0.01$; ***: $p < 0.001$; n.s.: not significant.

Representational processing coupled to the up-state of slow oscillations predicted successful memory for untested items

Electrophysiological and computational models suggest that slow oscillation (SO) up-state provides a critical time window for memory consolidation-related neural processing during sleep (Batterink et al., 2016; Ngo & Staresina, 2022; Wei et al., 2016) (see Fig. 4A). We next examined the relationship between item-specific representation, memory consolidation and SO phases. We filtered raw EEG signals in the frequency range of 0.3-1.25 Hz for subsequently remembered items at the Fz, wherein prominent SOs were observed (Batterink et al., 2016; Helfrich et al., 2018). For each participant, we then applied the Hilbert transformation to extract the instantaneous phases of SOs and computed the empirical coupling index between the SO phase and the concurrent representational strength (i.e., WI similarity) using the weighted Phase Locking Factor (wPLF) (Maris et al., 2011). The surrogate coupling index was generated by shuffling the corresponding relationship between the empirical phase and representational strength (see Methods). We found that for remembered items, empirical coupling indices were significantly greater than the surrogate coupling indices ($t(32) = 2.37$, $p = 0.024$, Fig. 4B), suggesting a significant coupling between representational strength and SO phase. We further examined whether the distribution of phases followed a non-uniform or uniform distribution across participants using the Rayleigh Z test. We found that the preferred phases were significantly clustered around the peak of the SO ($z = 6.06$, $p = 0.002$; mean vector length (*mlv*) = 0.43, preferred phase: 1.73°; Fig. 4C). In contrast, for subsequently forgotten items, there were neither significant coupling effects between representational strength and the phase of SO ($t(32) = 0.54$, $p = 0.592$) nor phase clustering ($z = 2.25$, $p = 0.105$; *mlv* = 0.26, preferred phase: 35.55°; see Fig. S6). No significant difference was found between the coupling strengths for subsequently remembered versus forgotten items ($t(32) = 1.26$, $p = 0.217$).

We next investigated whether pre-sleep testing modulated the observed coupling effect for remembered items by separating tested and untested items. We found that, for subsequently remembered tested items, the coupling was not significant ($t(32) = 1.37$, $p = 0.181$), while the preferred phases were marginally clustered around the peak of the SO ($z = 2.87$, $p = 0.055$; $mlv = 0.30$, preferred phase: -1.29°) (Fig. 4D-E). In contrast, for subsequently remembered untested items, representational strength was significantly coupled to the phase of SO ($t(32) = 3.00$, $p = 0.005$), with a preferred phase around the SO peak (i.e., up-state, $z = 4.50$, $p = 0.01$; $mlv = 0.37$, preferred phase: -2.50°) (Fig. 4F-G). However, there was no significant pre-sleep testing (tested vs. untested) by coupling index (empirical vs. surrogate) interaction effect ($F(1,32) = 2.27$, $p = 0.142$). These results suggested that the coupling between representational strength and the phase of SO for subsequently remembered items was mainly driven by the untested items.

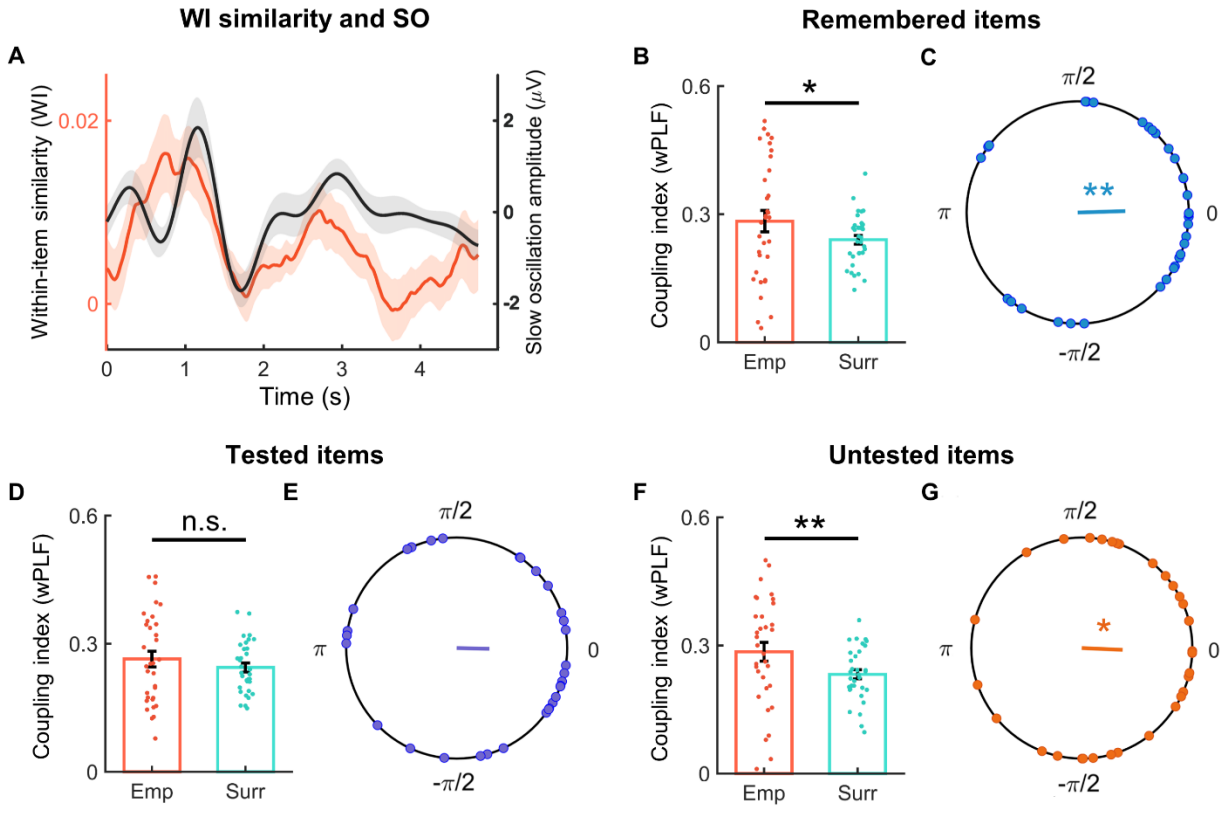

Fig 4. Representational processing was coupled to continuous slow oscillations (SOs) for subsequently remembered, untested items. (A) Grand average of representational strength (i.e., WI similarity, orange line) within the 5s following TMR cue onset across participants and the concurrent SOs filtered between 0.3-1.25 Hz. **(B-C)** Representational strength was coupled to the up-state of SOs in the Fz channel for subsequently remembered items. **(D-E)** Neither the coupling effect nor the phase clustering was significant for subsequently remembered tested

items. **(F-G)** Both the coupling effect and the phase clustering were significant for subsequently remembered untested items. *: $p < 0.05$; **: $p < 0.01$; n.s.: not significant.

Spindles predicted memory consolidation for untested items

Research suggests that TMR-based memory consolidation is tightly linked with post-cue spindle activity (Antony et al., 2018; Cairney et al., 2018). However, whether pre-sleep testing would modulate the spindle activity in supporting memory consolidation remains unclear. To address this question, we extracted spindles on individual trials (see Fig. 5A and Methods) and calculated spindle probability for each time point (Antony et al., 2018). Pre-sleep testing (tested vs. untested) by subsequent memory (remember vs. forget) repeated measures ANOVA was conducted across individual time points and found a significant interaction effect during 2352-3020 ms, $p_{corr} = 0.009$ (Fig. 5B). Note that only 32 participants were included in this analysis because one participant had no forgotten trials among tested items. Post-hoc comparisons showed that, among tested items, the spindle probability for remembered items was not different from the spindle probability for forgotten items ($t(31) = -2.08$, $p_{FWER} = 0.138$, Fig. 5C). In contrast, among the untested items, spindle probability for remembered items was greater than that for forgotten items ($t(31) = 3.46$, $p_{FWER} = 0.005$). Moreover, among those subsequently remembered items, untested items elicited higher spindle probability than the tested item ($t(31) = 3.77$, $p_{FWER} = 0.002$). We next examined the duration and onset of spindles from the first 2s to ensure that the increased spindles for subsequently remembered untested items during the 2352-3020 ms were not due to the longer duration or delayed onset of the early spindles (ps > 0.399, see Fig. S7). Moreover, in the 2352-3020 ms interaction time window, subsequently remembered untested items elicited higher spindle probability than the control cues ($t(32) = 2.27$, $p = 0.030$, Fig. S8), while no significant difference was found between the subsequently remembered tested items and control cues ($t(32) = -0.59$, $p = 0.561$). In addition, spindles centered during this interaction cluster were significantly coupled to the up-state of SOs for all tested and untested items ($ps < 0.015$) (see Fig. S9). Taken together, these results suggested that enhanced spindles support successful memory consolidation but only among untested items.

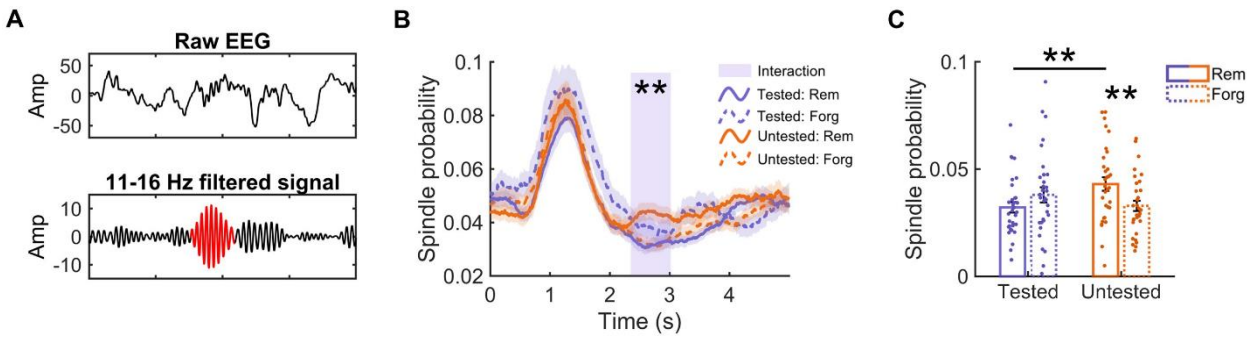

Fig 5. Spindles following TMR cues and the relationship between spindles and subsequent memories. (A) Spindle detection. Top: raw EEG data; Bottom: EEG signals filter between 11-16 Hz. A detected spindle event is highlighted in red. **(B)** Significant interaction effect between pre-sleep testing (tested vs. untested) and subsequent memory effect (remembered vs. forgotten items) on the spindle probability in the 2352-3020 ms cluster (highlighted in a shaded rectangle) post TMR cues. **(C)** Post-hoc analysis for the interaction effect (shaded rectangle in B). For tested items, the spindle probability elicited for post-sleep remembered items was not different from the spindle probability for forgotten items. In contrast, for untested items, post-sleep remembered items elicited greater spindle probability than forgotten items. In addition, the spindle probability for the subsequently remembered untested items was greater than that for the subsequently remembered tested item. **: $p < .01$.

Spindle activity coordinated item-specific memory reactivation for successfully remembered untested items

Our results thus far revealed that item-specific memory reactivation (2440-2960 ms in Fig. 3C) and increased spindles (2352-3020 ms in Fig. 5B) tended to co-occur in the late, highly overlapping time windows, with both indices implicated in memory consolidation for untested items. Importantly, spindles have been shown to temporally coordinate memory reactivation during NREM sleep (Antony et al., 2018; Cairney et al., 2018). Therefore, we next examined how spindles would predict item-level memory reactivation and subsequent memories in the overlapping time window (i.e., 2440-2960 ms), for tested and untested items, respectively. Among tested items, the linear mixed-effect model revealed that no significant effects were found for either subsequently remembered or forgotten items (ps > 0.577, Fig. 6A). In contrast, among untested items, the cue-elicited spindle probability positively predicted item-specific memory reactivation for subsequently remembered items ($\beta = 0.21$, $t(299) = 2.21$, $p = 0.028$, Fig. 6B) but not for forgotten items ($\beta = -0.08$, $t(489) = -0.89$, $p = 0.374$). Moreover, among untested

items, the prediction effect for remembered items was significantly greater than that for forgotten items ($\beta = 0.29$, $t(788) = 2.20$, $p = 0.028$).

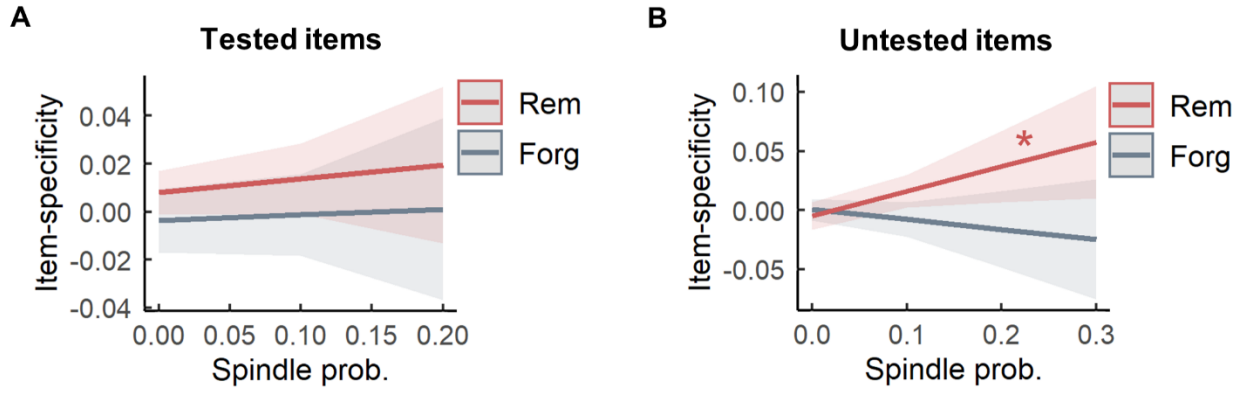

Fig 6. The relationship between spindles and item-specific memory reactivation in the overlapped late time window (i.e., 2440-2960 ms relative to cue onset). Among tested items, the spindle probability did not predict the item-specific memory reactivation for either subsequently remembered or forgotten items **(A).** In contrast, among untested items, the spindle probability significantly predicted the item-specific memory reactivation for subsequently remembered items but not for forgotten items **(B)**. *: $p < .05$.

Discussion

We asked fundamental yet unanswered questions in memory consolidation: how specific memories are reactivated during post-learning slow-wave sleep and how this supports memory consolidation? By applying multivariate representational similarity analyses (RSA) to targeted memory reactivation (TMR)-elicited EEG signals, we identified item-specific representations, which extends existing studies that show memory reactivation at a categorical level (e.g., Cairney et al., 2018; Shanahan et al., 2018; Wang et al., 2019). Moreover, our results support a temporally segregated memory reactivation account: during SWS, memory cues first elicited early item-specific representations, which primarily reflect the processing of individual cues. In a late time window, the item-specific representations contained specific memory traces, which contributed to post-sleep memory retention. Moreover, pre-sleep memory testing modulated the neural mechanisms underlying TMR, such that only among untested items, item-specific representations were supported by spindles and were temporally coupled to the up-state of SOs (see Fig. 7).

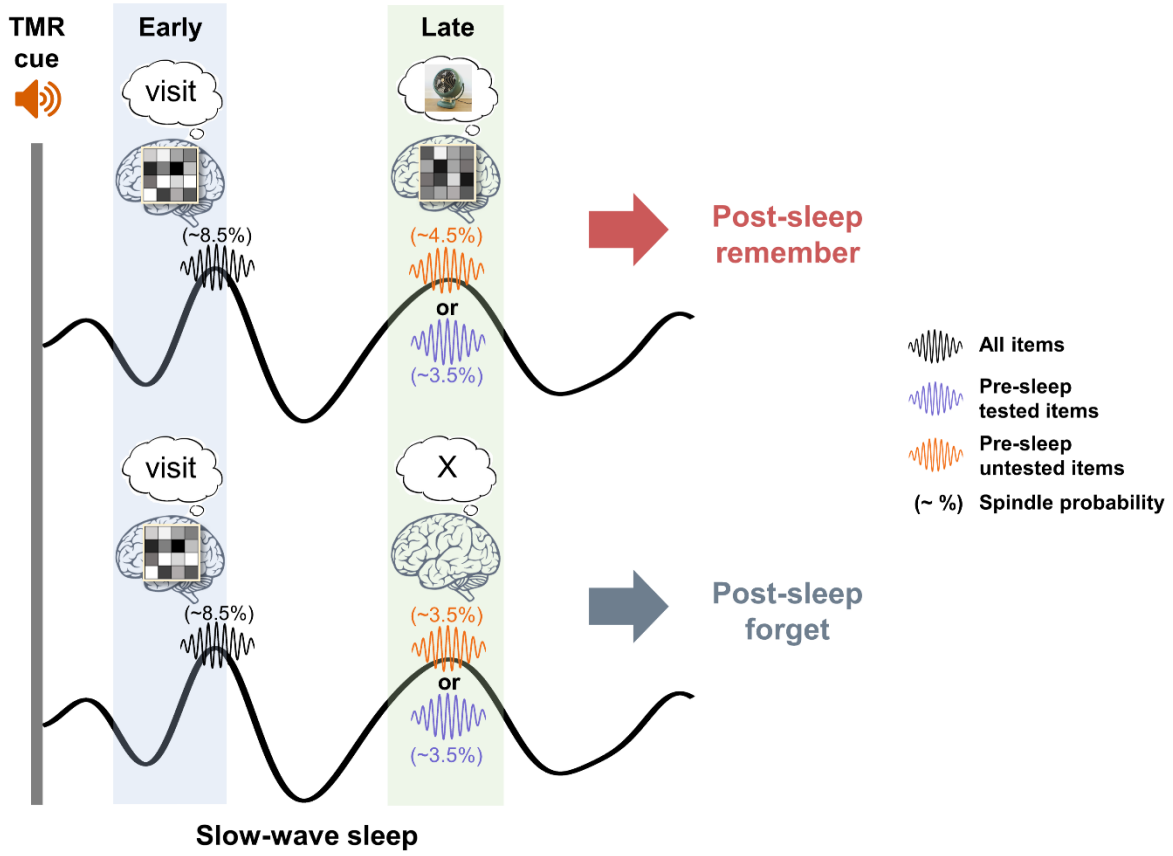

Fig 7. Item-specific memory reactivation following TMR cues promotes memory consolidation (schematic depiction). Re-presenting memory cues during slow-wave sleep trigger the item-specific representations of the sensory cues in an early time window. The TMR cue-elicited sensory-driven representations and the spindles in the early time window do not differ between post-sleep remembered and forgotten items. The sensory cues lead to further reactivations of item-specific representations in a late time window that contributes to memory consolidation and results in remembering in the post-sleep tests. In contrast, the sensory cues failed to reactivate the associated content leading to post-sleep forgetting. Moreover, the memory reactivation in the late time windows is modulated by the pre-sleep testing. Only for the untested items, the item-specific representation in the late cluster is supported by the increased spindle activities. The spindles and the memory reactivation processing are coupled to the up-state of the slow oscillations.

During the SWS, the sleeping brain continues to process external sensory information, which is a prerequisite for cue-triggered memory reactivation (Andrillon & Kouider, 2020). For example, non-human primate and rodent studies have shown that the neuronal responses of the primary auditory cortex are well preserved during sleep with little modulation by different vigilance states (Issa & Wang, 2008; Nir et al., 2015). Human research shows that the sleeping brain can

process meaningful auditory stimuli such as participants' own names (Perrin et al., 1999), voices (Ameen et al., 2022), lexical sounds (Kouider et al., 2014), continuous speech (Legendre et al., 2019), and new semantic associations (Xia et al., 2022; Züst et al., 2019). At the neural level, auditory stimulation during NREM sleep is manifested by increased EEG power in both the low-frequency range (2-10 Hz) and sigma band (11-16 Hz) immediately following auditory stimuli (Andrillon et al., 2016; Wislowska et al., 2022). Our results showed a highly similar pattern: TMR cues elicited increased low-frequency activities (1-10 Hz), followed by the extended sigma band activities (11-19 Hz) within approximately the first 2-s post cue onset, indicating the processing of sensory stimuli during sleep.

Beyond the spectral power changes, multivariate RSA revealed that cue-elicited EEG contained item-specific representations in this early cluster, which reflects the initial processing of specific memory cues. Indeed, this early item-specific representation was identified not only for all memory cues regardless of subsequent memory performance, but also for control cues without any memory associations. This early, effective processing of memory cues would potentially reactivate their associated, hippocampus-dependent memory traces (Diekelmann et al., 2011; McClelland et al., 1995; Rasch et al., 2007; Squire, 1992). Reactivated hippocampal memory traces then trigger pattern completion and the reinstatement of the neocortex-dependent memory representations (Rolls, 2013; Staresina & Wimber, 2019). Correspondingly, we found a late time window showing item-specific representations, which were associated with the post-sleep memory. The sequential item-specific representations of memory cues and their associated memory content are consistent with the recently proposed TMR-based memory consolidation framework, which proposes sensory- and hippocampus-driven memory reactivation (Lewis & Bendor, 2019).

Item-specific memory reactivation following TMR cues could be achieved via a cortical-hippocampal-cortical loop (Berkers et al., 2018; Rothschild et al., 2017), which is observed during sleep in both humans and rodents and served as the foundation for systems memory consolidation (Helfrich et al., 2019; Klinzing et al., 2019; Maingret et al., 2016; Mitra et al., 2016; Ngo et al., 2020). During sleep, this cortical-hippocampal-cortical loop is supported by the coupling of the thalamocortical spindles to the up-state of neocortex-originated slow oscillations, which may constitute an optimal time window for cross-regional communications and memory

consolidation (Helfrich et al., 2019; Ngo et al., 2020; Schreiner et al., 2021). Intriguingly, our results showed that item-specific memory reactivation in the late time window was accompanied by increased spindles, especially for successfully remembered untested items. Moreover, both TMR-elicited representational reactivation strength and the increased spindles were preferentially coupled to the up-state of SOs. Together with recent evidence showing that SOs up-state is conducive to TMR-induced memory reactivation and sleep learning (Abdellahi et al., 2023; Batterink et al., 2016; Ngo & Staresina, 2022, 2022; Xia et al., 2022; Züst et al., 2019), our results indicating that SO up-state and concurrent spindles provide a privileged time window for memory reactivation and cross-regional information transfer. A precise delineation of the TMR-triggered cross-regional interaction awaits future investigations that employ neuroimaging methods affording both high spatial and temporal resolutions (e.g., MEG, iEEG, and simultaneously EEG-fMRI).

Regarding the role of spindles, we found substantial spindle and sigma power increases in an earlier time window (within the first 2s) following TMR cues, although this spindle activity was unrelated to the subsequent memory. These early cue-elicited spindles may reflect the protective mechanisms ensuring sleep is preserved even when perturbation happens (Halász et al., 2014). Increased spindle activity in the early time window was followed by decreased spindles, which constituted a spindle refractory period when spindles become less likely to occur and are instrumental for memory reprocessing and consolidation (Antony et al., 2018; Antony et al., 2019). Indeed, we found significant item-specific memory representations for subsequently remembered items during this refractory period, while the increased spindle activity for untested items as compared with tested items might reflect the preferential processing and consolidation of weakly memorized items (Denis et al., 2021).

Indeed, our results suggested that pre-sleep testing modulated the neural mechanisms underlying TMR-induced memory consolidation. First, cue-elicited neural activity within the first 2 s post cue onset positively predicted cueing benefits only for untested items. Second, for untested items, increased spindles in the late time window (2440-2960 ms) positively predicted long-term memory. Third, for subsequently remembered untested items, spindles in this late time window were positively correlated with their item-specific representations. These remarkable neural-behavior differences between tested and untested items could be due to different levels of

consolidation induced by pre-sleep testing. Specifically, pre-sleep retrieval could rapidly engage the medial prefrontal cortex while slowly decreasing hippocampus activity via hippocampal-neocortical interactions, thereby inducing fast systems consolidation during wakefulness (Antony et al., 2017). This fast systems-level consolidation could resemble sleep-mediated memory consolidation (Antony et al., 2017; Himmer et al., 2019). Thus, in subsequent sleep, TMR may not drive further consolidation for tested items (Joensen et al., 2022). Our findings indicated that TMR preferentially consolidates untested items during sleep, which complements memory consolidation during wakefulness.

Although previous studies showed significant TMR benefits for associative memory (see Hu et al., 2020), our study found numerical but nonsignificant TMR benefits for untested items (see Fig. S1A). A few possibilities might account for the absence of TMR benefits. First, our pre-sleep learning session included repeated encoding and mental rehearsal, which may attenuate the TMR benefits. Specifically, in a previous study using a similar word-picture paradigm, participants learned each word-picture association twice (Cairney et al., 2018). In contrast, participants in our study learned fewer word-picture pairs, while each pair was repeated three times. Additionally, after the encoding phase, participants were encouraged to visualize and maintain the target picture in their minds while hearing the spoken cue words. Repeated mental rehearsal might contribute to fast consolidation, which could weaken the TMR benefits during sleep (Antony et al., 2017). Corroborating this possibility, several studies have shown that TMR benefits were more pronounced for weakly encoded items (Cairney et al., 2016; Creery et al., 2015). Second, more precise memory measurements are desirable to detect the TMR benefits, such as the error distance measure used in previous TMR spatial memory research (Rasch et al., 2007; Rudoy et al., 2009). Future word-picture or naturalistic episodic memory should include measures such as verbal recall to test both perceptual and conceptual details.

In conclusion, our findings contributed to the mechanistic understanding of how external cueing during NREM sleep promoted memory consolidation. We identified that TMR cues reactivated item-specific representations in segregated early and late time windows. Importantly, pre-sleep testing modulated the underlying neural mechanisms: for untested items, enhanced spindles in the late time window supported item-specific representations and memory consolidation. We

also found that the strength of representational reactivation and spindles peaked at the SO up-states, a privileged time window for consolidation to occur.

Methods

Participants

Thirty-three healthy, right-handed participants were included in the analyses (25 females, mean ± SD age, 21.91 ± 2.65 years). Four additional participants were recruited, yet their data were excluded because they received fewer than three rounds of TMR trials (*a priori* criterion to ensure signal-to-noise ratio of EEG analyses) due to insufficient or unstable N2 and N3 sleep. All included participants had normal or corrected-to-normal vision. Participants were prescreened on sleep by using the questionnaires including the Pittsburgh Sleep Quality Index (PQSI) and the Insomnia Severity Index (ISI). They all reported overall good sleep quality and had not taken any medicines to aid sleep in the past month before the experiment. All participants did not suffer from any neurological or psychiatric disorders. The study was approved by the Research Ethics Committee of the University of Hong Kong. All participants gave written informed consent prior to the experiment.

Stimuli

A total of 96 two-character Chinese verbs and 96 target pictures were used in the experiment. Each verb was randomly paired with a complex visual picture, resulting in 96 cue (word)-target (picture) pairs. The central element of each picture was from one of four categories (i.e., animals, electronic devices, plants, and transportation tools), with 24 pictures in each category. For each picture, a highly similar picture was also selected and served as a lure in the old/new recognition task. For each unique picture, the target and lure were randomly assigned among participants. For verbs, visually presented verbs were only used in the familiarization phase, while aurally presented verbs were used throughout the entire experiment. Four additional two-character Chinese verbs were presented during the familiarization phase but were never paired with any pictures. These verbs served as control cues in the TMR. Auditory sounds of the verbs were generated using the Text-To-Speech of iFLYTEK, with an average duration of 631.70 ms (SD: 55.40 ms).

Procedure

All participants arrived at the sleep lab around 8:30 pm. Participants completed the following tasks in order: a vigilance task, a stimuli familiarization task, a cue-target associative learning task, and a pre-sleep memory test. Participants then proceeded to sleep (12 am to 8 am the next morning), wherein TMR was administered during slow-wave sleep. After ~30 min upon wakening, participants' vigilance levels were assessed again, followed by the post-sleep memory test.

Psychomotor vigilance task

Participants' vigilance levels were assessed using the Psychomotor Vigilance Task (PVT), right after participants arrived at the sleep lab and the next day morning. During the vigilance task, a fixation was presented on the center of the screen with a jitter duration in the range of 2-10 s. Then, the fixation was replaced by a counter counting incrementally from 0 in 10 ms increments. Participants were instructed to stop the counter by pressing the space bar immediately after they detected the change of fixation to the number. Response time that appeared on the screen would serve as feedback on the performance. This task lasted for 5 minutes.

Cue word and picture familiarization task

The familiarization task consists of two sessions, a word-familiarization session, and a picture-familiarization session. In the word-familiarization session, each trial started with a 0.3 s fixation, followed by a 0.5 s blank screen. Afterward, a verb was visually presented on the center of the screen for 2 s, accompanied by its verbalization from the speaker. Participants judged whether the spoken verbs were clear and recognizable by pressing a button. All 100 verbs (96 verbs in the word-picture pairs and 4 verbs as control stimuli) were randomly presented during this stage, with each verb being presented twice. In the picture familiarization session, each trial started with 0.3 s fixation, followed by a 0.5 s blank screen. Afterward, a picture and its label (e.g., for a panda picture, the label would be "panda") were presented on the screen for 2 s. Participants indicated whether they were familiar with the picture and its name by pressing a button. Each of the 192 pictures (96 targets + 96 lures) was presented twice. Participants indicated that all stimuli were clearly recognizable and familiar after the familiarization task.

Word-picture associative learning task

Participants learned 96 word-picture pairs. Each learning trial consisted of three phases, an encoding phase, a maintenance phase, and a vividness rating phase. During the encoding phase, following a 0.3 s fixation and a black screen jittering between 0.9-1.5 s, participants viewed a picture presented in the center of the screen for 2 s while hearing the spoken verb from the speaker. Participants were instructed to pay attention to the details of the picture while memorizing the verb-picture associations during the encoding phase. During the maintenance phase, the picture disappeared, and participants were asked to maintain the picture in their minds as vividly as possible for 3s while hearing the spoken verb again. In the vividness rating phase, participants indicated the vividness of the mental image of the picture on a 1 (not vivid at all) -4 (very vivid) point Likert scale by pressing one of four buttons. The learning task consisted of three blocks, with each block containing 32 unique verb-picture pairs that were repeated three times. To reduce the recency effect, participants completed a ~5 min math task after the learning task.

Pre-sleep memory test

To understand whether the pre-sleep testing alters TMR benefits on memory consolidation, participants were tested on half of the pairs during the pre-sleep test (i.e., 48 pairs, with 12 pairs from one of the four picture categories). This test consisted of a cued recall task and a cued recognition task.

In the cued recall task, each trial started with a 0.3 s fixation, followed by a blank screen (0.9-1.5 s). The spoken verb was played, prompting participants to report whether they could “remember” or “forget” the corresponding picture. This stage was self-paced so that participants had enough time to recall. Immediately following this “remember” or “forget” response, participants were further asked to report the category of the picture by pressing one of four buttons, with each button indicating one of four categories within 2 s.

The same half of the pairs were tested in the cued-recognition task. Each trial started with a fixation (0.3 s) and was followed by a blank screen (0.9-1.5 s). Participants next saw the picture presented on the center of the screen while hearing the spoken verb. Participants were asked to indicate if the picture was the same picture paired with the verb during the previous learning task by pressing the “Yes” or “No” button. Among 192 recognition trials, 48 trials showed identical

verb-picture associations from the learning task, and 48 trials showed verb-lure picture associations. The remaining 96 trials consisted of 48 mixed verb-picture associations and 48 mixed verb-lure associations with cue verbs and pictures (or lures) corresponding to different learning trials.

TMR during NREM sleep

To counterbalance the pre-sleep memory performance between cued and uncued items, we selected half of the remembered and half of the forgotten pairs (based on the category report performance in the cued recall task) of the tested items as cued items during TMR. In addition, we randomly selected half of the untested items to be cued in the TMR. Picture categories were balanced across cued versus non-cued conditions. Thus, the TMR session contained 48 verbs as cues, with additional 4 verbs that were not paired with any pictures as control cues. Half of the cues were from tested trials, with the remaining half from untested trials. The control cues served as the baseline to examine retrieval-specific neural activity. Therefore, there were 52 unique sound cues played during sleep.

During the nocturnal sleep, white noise was played in the background throughout the night, with an intensity of ~ 45 dB, measured by a sound-level meter placed at the same position where participants laid their heads on the pillow. Experienced experimenters monitored the EEG signals and visually identified signature EEG events characterizing different sleep stages (e.g., spindles, K-complex, slow oscillations). Upon detecting stable slow-wave sleep, the experimenter would begin the TMR, which occurred ~50.18 min (SD: 35.38 min) after the start of the sleep phase. On average, participants were presented with 8.44 (SD: 3.49) rounds of TMR. In each round of TMR, 52 verb cues were randomly presented with an inter-stimuli interval of 5 ± 0.2 s. After each round of cueing, the order of the TMR cues was shuffled and replayed again. Each round was separated by 30 s. The TMR session continued as long as the participants were in slow-wave sleep in the first 3-4 hours of the nocturnal sleep. Cueing was stopped immediately when participants showed signs of micro-arousals, awakening or changed to N1 sleep or rapid eye movement (REM) sleep. Cueing was resumed after the participants returned to stable slow-wave sleep.

Post-sleep memory test

Approximately 30 minutes after awakening and after the PVT test, participants were tested on all 96 pairs. Similar to pre-sleep memory tests, this test included the cued recall and cued recognition tasks. In addition, there was a closed-eye mental retrieval task between these two tasks, in which participants were asked to keep their eyes closed and relax while each of the verbs was randomly played via the speaker (ISI = 5 ± 0.2 s). Upon hearing the verb, participants were asked to mentally retrieve the corresponding picture and keep the picture in their minds as vivid as they could until the next verb. If they could not remember the picture, they were told to keep their minds blank.

EEG recording and preprocessing

We collected the EEG data throughout the experiment except for during the familiarization and PVT tasks. EEG data were recorded using the amplifier from the eego system (ANT neuro, Netherlands, https://www.ant-neuro.com) with a sampling rate of 500 Hz from 61 channels (waveguard EEG caps) that were mounted in the International 10-20 system. Additionally, there were two electrodes placed on the left and right mastoids, respectively, and one electrode was placed above the left eye for the EOG measurements. Online EEG recordings were referenced to the default reference channel (i.e., CPz). For sleep monitoring, another two electrodes were placed on both sides of the chin to measure the EMG using the bipolar reference. EEG data collection was started after the impedance of all electrodes was lower than 20KΩ.

Sleep EEG data preprocessing was performed using EEGLAB (https://sccn.ucsd.edu/eeglab/) and Fieldtrip toolboxes (Oostenveld et al., 2011), as well as in-house code that was implemented in MATLAB (MathWorks Inc.). EEG data were first notch filtered at 50 ± 2 Hz, and then bandpass filtered between 0.5 and 40 Hz. Then continuous sleep EEG data were segmented into 15 s epochs, i.e., form -5 s to 10 s relative to the onset of TMR cues. This long epoch was used to eliminate the edge effect in the later time-frequency analysis. Our main interesting time windows for the sleep data are from 0 to 5 s relative to the TMR cue onset. Bad epochs are marked based on visual inspection and rejected from further analysis. Bad channels were marked and interpolated using spherical interpolation in EEGLAB. Afterward, EEG data were re-referenced to the average of the artifact-free data.

Time-frequency analysis

We performed time-frequency transformation on the preprocessed EEG data, using the complex Morlet wavelets (six cycles). Spectral power was extracted from the frequency range of 1-40 Hz, with a step of 1 Hz and with the time of interest range of [-1 5 s] relative to the TMR cue onset. The power was down-sampled to 100 Hz after the time-frequency transformation. We normalized the power data within each frequency bin and each channel by first subtracting the mean power in the baseline time windows ([-1 -0.5s] relative to the TMR cue onset) and then dividing the same baseline mean power. Finally, we re-segmented the power data into the 5s epochs (i.e., [0 5s] relative to the TMR cue onset).

Spindle detection

Individual spindles were detected during the TMR periods following previous studies (Antony et al., 2018). Specifically, artifact-free EEG data during the TMR periods were first bandpass filtered between 11-16 Hz by using the 4th order two-pass Butterworth filter. Next, the root-mean-square (RMS) values were calculated for each time point with a moving window of 400 ms. Third, the spindle amplitude criterion is defined as the mean + 1.5 SD of the RMS signal. Sleep spindles were detected if the RMS signal consecutively exceeded the amplitude criterion for a duration of 0.5 to 3 s. Previous studies indicated that spindle activity was prominent over anterior-posterior midlines (Dehghani et al., 2011). To this end, spindle detection was performed for all seven midline EEG channels (i.e., “FPz”, ”Fz”, ”FCz”, ”Cz”, ”Pz”, ”POz”, and “Oz”), separately. We then assign the spindle value of 1 to the time points where a spindle was detected and 0 otherwise. The spindle probability was computed as the mean spindle values across trials for each time point in the time range of [0 5 s] relative to the TMR cue onset and then averaged across all midline channels.

Slow-oscillation detection

The detection of slow oscillations (SOs) was performed on the artifact-free EEG data during the TMR periods. We first bandpass filtered the EEG data between 0.3 and 1.25 Hz using the two-pass FIR filter, with the order equaling the three cycles of the low-frequency cut-off. We then detected the zero-crossings in the filtered signal, and the event durations were calculated as the temporal distance between two successive positive-to-negative zero-crossings. SO was detected if the peak-to-peak amplitude was greater than the 75% percentile of the absolute amplitude of

the filtered signal (Helfrich et al., 2018) and the event duration was between 0.8 s and 2 s. SOs detection was performed on the Fz, where the amplitude of SOs was prominent according to previous studies (Marshall et al., 2006).

SO-spindle coupling

For TMR trials that showed both the spindle and SOs in the time windows (i.e., 2440-2960 ms), which showed significant interactions of item-specificity and memory effect, we then performed the SO-spindle coupling. We first filtered the SO-spindle trials in the SO frequency range (i.e., 0.3-1.25 Hz). We then applied the Hilbert transform to the filtered data to extract the instantaneous phase of the SOs. To obtain the amplitude of the spindle activities, we filtered the SO-spindle trials in the spindle frequency range (i.e., 11-16 Hz) and then applied the Hilbert transform to the filtered data to obtain the instantaneous amplitude of the spindle activities on an extended time window (i.e., [2-4 s] relatively to TMR cue onset to ensure at least half of the SOs cycle was included). We detected the preferred SO phase, which is concurrent with the maximal spindle amplitude across all trials in each participant, and then tested the distribution of the preferred SO phases across participants against the uniform distribution using the Rayleigh test (CircStat toolbox, Berens, 2009).

Representational similarity analysis

To extract item-specific representations, we performed representational similarity analysis (RSA) between every two clean TMR trials that originated from different TMR rounds. Specifically, the within-item similarity was calculated as the whole-brain EEG cortical pattern similarity between the same TMR cues; and the between-item similarity was calculated as the pattern similarity between different TMR cues. Thus, contrasting within-item similarity versus between-items similarity enables us to examine whether there are item-specific representations following the TMR cues.

To characterize the item-specific representations across time, RSA was performed on the preprocessed raw EEG using sliding time windows of 500 ms, with an incremental step of 10 ms, resulting in 250*61 (time points * channels) features in each time window. Then, for each time window, we calculate the similarity between vectorized features of every two trials that were

from different TMR rounds using Spearman's corrections. All the correlation values were Fisher *Z*-transformed before further statistical analysis.

Coupling between representational strength and SOs

To get rid of the effect of the potential non-normalized magnitude of representational strength on the coupling index, we measured the coupling between the memory reactivation strength and phase of slow oscillatory activity by a weighted phase-locking factor (wPLF) (Maris et al., 2011). Specifically, for each subject, within-item similarity values indexing the representational strength of individual items were first extracted across the 5 s periods following the TMR cue onset. The WI similarity values were then mean-centered and normalized. Meanwhile, the continuous SOs were obtained by bandpass filtering the raw EEG data between 0.3 and 1.25 Hz using the two-pass FIR filter, with the order equaling the three cycles of the low-frequency cut-off. We then computed the concurrent SOs for every single subject by averaging the SOs across the same trials that were used to obtain the WI similarity. The SOs were then Hilbert transformed to extract the phase values. We then computed the inner product between the time-varying WI similarity values and phase values, resulting in a complex number, the magnitude of which indicated the coupling strength and the phase of which showed the preferred phase angle where consolidation-related neural representations occurred. The surrogate coupling index for each participant was obtained by scrambling the phase using the inverse FFT while preserving the power spectrum of the signal and then calculating the coupling index between the scrambled phase and WI similarity values. Of note, the surrogate index was computed 100 times and then averaged for each participant. The significance of coupling was examined by contrasting the empirical coupling index with the averaged surrogate coupling index across participants.

Instead of qualitatively describing the preferred phase, which was extracted from the averaged complex number across participants, we statically tested the preferred phase of consolidation-related processing of neural representations regardless of the representational strength in an independent phase clustering analysis. Specifically, we extracted the preferred phase for individual participants and then tested the distribution of the preferred phases against the uniform distribution using the Rayleigh test (CircStat toolbox) across all participants.

Statistics

For the behavioral data, we conducted a two-way ANOVA with TMR benefits (cued vs. uncued) and pre-sleep testing (tested vs. untested) as repeated measures in analyzing the post-sleep memory performance. We also performed a two-way ANOVA with TMR and time (pre-sleep vs. post-sleep) as repeated measures in analyzing the memory performance for tested items. The paired sample *t*-tests were employed to examine the differences between two specific experimental conditions (e.g., memory performance between pre-sleep tested items and post-sleep tested items). The relationship between EEG activities during the TMR period and post-sleep memory performance is assessed by the robust linear regression model, which is less likely to be affected by potential outliers (Yu & Yao, 2017).

For the EEG data, multiple comparisons across consecutive time windows were corrected using the cluster-based nonparametric statistical tests in MATLAB (Maris & Oostenveld, 2007). Specifically, statistical tests (e.g., *t*-test) were performed between conditions (e.g., WI vs. BI or tested vs. untested) in individual time (or time-frequency) windows. Adjacent time (or time-frequency) windows with statistical values exceeding a threshold ($p < 0.05$) were combined into contiguous clusters. Cluster-level statistics were computed using the sum of the *t* values within a cluster. To test the significance of the time (or time-frequency) cluster, a distribution of cluster-level statistics under the null hypothesis was constructed by randomly permuting condition labels 1000 times, and the maximum cluster-level statistic in each permutation was extracted. If no significant cluster was found for a permutation, a value of 0 was assigned for that permutation. The nonparametric statistical significance of a cluster was then obtained by calculating the proportion of cluster-level statistics in the distribution under the null hypothesis that exceeded the empirical cluster-level statistics. For an identified cluster, we also performed a two-way ANOVA with item-specificity (WI vs. BI similarity) and pre-sleep testing as repeated measures and a two-way ANOVA with item-specificity and subsequent memory as repeated measures. The statistical significance level for all the analyses is set as *p*-value < .05 or corrected *p*-value (p_{corr}) < 0.05.

Acknowledgment

General: We thank Lingqi Zhang and Zexuan Mu for their help with the data collection.

Funding: The research was supported by the Ministry of Science and Technology of China STI2030-Major Projects (No. 2022ZD0214100), National Natural Science Foundation of China (No. 32171056), General Research Fund (No. 17614922) of Hong Kong Research Grants Council, and the Key Realm R&D Program of Guangzhou (No. 20200703005) to X. H., General Research Fund (No. 17600621) of Hong Kong Research Grants Council to T. L., and Start-up Fund for RAPs under the Strategic Hiring Scheme at The Hong Kong Polytechnic University (Project ID: P0043338) to J. L.

Competing interests: The authors declare no compete of interests.

References

Abdellahi, M. E. A., Koopman, A. C. M., Treder, M. S., & Lewis, P. A. (2023). Targeting targeted memory reactivation: Characteristics of cued reactivation in sleep. *NeuroImage*, *266*, 119820. https://doi.org/10.1016/j.neuroimage.2022.119820

Ameen, M. S., Heib, D. P. J., Blume, C., & Schabus, M. (2022). The Brain Selectively Tunes to Unfamiliar Voices during Sleep. *Journal of Neuroscience*, *42*(9), 1791–1803. https://doi.org/10.1523/JNEUROSCI.2524-20.2021

Andrillon, T., & Kouider, S. (2020). The vigilant sleeper: Neural mechanisms of sensory (de)coupling during sleep. *Current Opinion in Physiology*, *15*, 47–59. https://doi.org/10.1016/j.cophys.2019.12.002

Andrillon, T., Poulsen, A. T., Hansen, L. K., Léger, D., & Kouider, S. (2016). Neural Markers of Responsiveness to the Environment in Human Sleep. *Journal of Neuroscience*, *36*(24), 6583–6596. https://doi.org/10.1523/JNEUROSCI.0902-16.2016

Antony, J. W., Ferreira, C. S., Norman, K. A., & Wimber, M. (2017). Retrieval as a Fast Route to Memory Consolidation. *Trends in Cognitive Sciences*, *21*(8), 573–576. https://doi.org/10.1016/j.tics.2017.05.001

Antony, J. W., Piloto, L., Wang, M., Pacheco, P., Norman, K. A., & Paller, K. A. (2018). Sleep Spindle Refractoriness Segregates Periods of Memory Reactivation. *Current Biology*, *28*(11), 1736-1743.e4. https://doi.org/10.1016/j.cub.2018.04.020

Antony, J. W., Schönauer, M., Staresina, B. P., & Cairney, S. A. (2019). Sleep Spindles and Memory Reprocessing. *Trends in Neurosciences*, *42*(1), 1–3. https://doi.org/10.1016/j.tins.2018.09.012

Batterink, L. J., Creery, J. D., & Paller, K. A. (2016). Phase of Spontaneous Slow Oscillations during Sleep Influences Memory-Related Processing of Auditory Cues. *Journal of Neuroscience*, *36*(4), 1401–1409. https://doi.org/10.1523/JNEUROSCI.3175-15.2016

Belal, S., Cousins, J., El-Deredy, W., Parkes, L., Schneider, J., Tsujimura, H., Zoumpoulaki, A., Perapoch, M., Santamaria, L., & Lewis, P. (2018). Identification of memory reactivation during sleep by EEG classification. *NeuroImage*, *176*, 203–214. https://doi.org/10.1016/j.neuroimage.2018.04.029

Bendor, D., & Wilson, M. A. (2012). Biasing the content of hippocampal replay during sleep. *Nature Neuroscience*, *15*(10), Article 10. https://doi.org/10.1038/nn.3203

Berens, P. (2009). CircStat: A MATLAB Toolbox for Circular Statistics. *Journal of Statistical Software*, *31*, 1–21. https://doi.org/10.18637/jss.v031.i10

Berkers, R. M. W. J., Ekman, M., van Dongen, E. V., Takashima, A., Barth, M., Paller, K. A., & Fernández, G. (2018). Cued reactivation during slow-wave sleep induces brain connectivity changes related to memory stabilization. *Scientific Reports*, *8*(1), Article 1. https://doi.org/10.1038/s41598-018-35287-6

Born, J., & Wilhelm, I. (2012). System consolidation of memory during sleep. *Psychological Research*, *76*(2), 192–203. https://doi.org/10.1007/s00426-011-0335-6

Cairney, S. A., Guttesen, A. á V., El Marj, N., & Staresina, B. P. (2018). Memory Consolidation Is Linked to Spindle-Mediated Information Processing during Sleep. *Current Biology*, *28*(6), 948-954.e4. https://doi.org/10.1016/j.cub.2018.01.087

Cairney, S. A., Lindsay, S., Sobczak, J. M., Paller, K. A., & Gaskell, M. G. (2016). The Benefits of Targeted Memory Reactivation for Consolidation in Sleep are Contingent on Memory Accuracy and Direct Cue-Memory Associations. *Sleep*, *39*(5), 1139–1150. https://doi.org/10.5665/sleep.5772

Creery, J. D., Oudiette, D., Antony, J. W., & Paller, K. A. (2015). Targeted Memory Reactivation during Sleep Depends on Prior Learning. *Sleep*, *38*(5), 755–763. https://doi.org/10.5665/sleep.4670

Dehghani, N., Cash, S. S., & Halgren, E. (2011). Topographical frequency dynamics within EEG and MEG sleep spindles. *Clinical Neurophysiology*, *122*(2), 229–235. https://doi.org/10.1016/j.clinph.2010.06.018

Denis, D., Mylonas, D., Poskanzer, C., Bursal, V., Payne, J. D., & Stickgold, R. (2021). Sleep Spindles Preferentially Consolidate Weakly Encoded Memories. *Journal of Neuroscience*, *41*(18), 4088–4099. https://doi.org/10.1523/JNEUROSCI.0818-20.2021

Diekelmann, S., Büchel, C., Born, J., & Rasch, B. (2011). Labile or stable: Opposing consequences for memory when reactivated during waking and sleep. *Nature Neuroscience*, *14*(3), Article 3. https://doi.org/10.1038/nn.2744

Feng, K., Zhao, X., Liu, J., Cai, Y., Ye, Z., Chen, C., & Xue, G. (2019). Spaced Learning Enhances Episodic Memory by Increasing Neural Pattern Similarity Across Repetitions. *Journal of Neuroscience*, *39*(27), 5351–5360. https://doi.org/10.1523/JNEUROSCI.2741-18.2019

Fuentemilla, L., Miró, J., Ripollés, P., Vilà-Balló, A., Juncadella, M., Castañer, S., Salord, N., Monasterio, C., Falip, M., & Rodríguez-Fornells, A. (2013). Hippocampus-Dependent Strengthening of Targeted Memories via Reactivation during Sleep in Humans. *Current Biology*, *23*(18), 1769–1775. https://doi.org/10.1016/j.cub.2013.07.006

Halász, P., Bódizs, R., Parrino, L., & Terzano, M. (2014). Two features of sleep slow waves: Homeostatic and reactive aspects – from long term to instant sleep homeostasis. *Sleep Medicine*, *15*(10), 1184–1195. https://doi.org/10.1016/j.sleep.2014.06.006

Helfrich, R. F., Lendner, J. D., Mander, B. A., Guillen, H., Paff, M., Mnatsakanyan, L., Vadera, S., Walker, M. P., Lin, J. J., & Knight, R. T. (2019). Bidirectional prefrontal-hippocampal dynamics organize information transfer during sleep in humans. *Nature Communications*, *10*(1), Article 1. https://doi.org/10.1038/s41467-019-11444-x

Helfrich, R. F., Mander, B. A., Jagust, W. J., Knight, R. T., & Walker, M. P. (2018). Old Brains Come Uncoupled in Sleep: Slow Wave-Spindle Synchrony, Brain Atrophy, and Forgetting. *Neuron*, *97*(1), 221-230.e4. https://doi.org/10.1016/j.neuron.2017.11.020

Himmer, L., Schönauer, M., Heib, D. P. J., Schabus, M., & Gais, S. (2019). Rehearsal initiates systems memory consolidation, sleep makes it last. *Science Advances*, *5*(4), eaav1695. https://doi.org/10.1126/sciadv.aav1695

Hu, X., Cheng, L. Y., Chiu, M. H., & Paller, K. A. (2020). Promoting memory consolidation during sleep: A meta-analysis of targeted memory reactivation. *Psychological Bulletin*, *146*(3), 218–244. https://doi.org/10.1037/bul0000223

Issa, E. B., & Wang, X. (2008). Sensory Responses during Sleep in Primate Primary and Secondary Auditory Cortex. *Journal of Neuroscience*, *28*(53), 14467–14480. https://doi.org/10.1523/JNEUROSCI.3086-08.2008

Joensen, B. H., Harrington, M. O., Berens, S. C., Cairney, S. A., Gaskell, M. G., & Horner, A. J. (2022). Targeted memory reactivation during sleep can induce forgetting of overlapping memories. *Learning & Memory*, *29*(11), 401–411. https://doi.org/10.1101/lm.053594.122

Klinzing, J. G., Niethard, N., & Born, J. (2019). Mechanisms of systems memory consolidation during sleep. *Nature Neuroscience*, *22*(10), Article 10. https://doi.org/10.1038/s41593-019-0467-3

Kouider, S., Andrillon, T., Barbosa, L. S., Goupil, L., & Bekinschtein, T. A. (2014). Inducing Task-Relevant Responses to Speech in the Sleeping Brain. *Current Biology*, *24*(18), 2208–2214. https://doi.org/10.1016/j.cub.2014.08.016

Legendre, G., Andrillon, T., Koroma, M., & Kouider, S. (2019). Sleepers track informative speech in a multitalker environment. *Nature Human Behaviour*, *3*(3), Article 3. https://doi.org/10.1038/s41562-018-0502-5

Lewis, P. A., & Bendor, D. (2019). How Targeted Memory Reactivation Promotes the Selective Strengthening of Memories in Sleep. *Current Biology*, *29*(18), R906–R912. https://doi.org/10.1016/j.cub.2019.08.019

Liu, J., Zhang, H., Yu, T., Ren, L., Ni, D., Yang, Q., Lu, B., Zhang, L., Axmacher, N., & Xue, G. (2021). Transformative neural representations support long-term episodic memory. *Science Advances*, *7*(41), eabg9715.

Lu, Y., Wang, C., Chen, C., & Xue, G. (2015). Spatiotemporal Neural Pattern Similarity Supports Episodic Memory. *Current Biology*, *25*(6), 780–785. https://doi.org/10.1016/j.cub.2015.01.055

Maingret, N., Girardeau, G., Todorova, R., Goutierre, M., & Zugaro, M. (2016). Hippocampo-cortical coupling mediates memory consolidation during sleep. *Nature Neuroscience*, *19*(7), Article 7. https://doi.org/10.1038/nn.4304

Maris, E., & Oostenveld, R. (2007). Nonparametric statistical testing of EEG- and MEG-data. *Journal of Neuroscience Methods*, *164*(1), 177–190. https://doi.org/10.1016/j.jneumeth.2007.03.024

Maris, E., van Vugt, M., & Kahana, M. (2011). Spatially distributed patterns of oscillatory coupling between high-frequency amplitudes and low-frequency phases in human iEEG. *NeuroImage*, *54*(2), 836–850. https://doi.org/10.1016/j.neuroimage.2010.09.029

Marshall, L., Helgadóttir, H., Mölle, M., & Born, J. (2006). Boosting slow oscillations during sleep potentiates memory. *Nature*, *444*(7119), Article 7119. https://doi.org/10.1038/nature05278

McClelland, J. L., McNaughton, B. L., & O'Reilly, R. C. (1995). Why there are complementary learning systems in the hippocampus and neocortex: Insights from the successes and failures of connectionist models of learning and memory. *Psychological Review*, *102*, 419–457. https://doi.org/10.1037/0033-295X.102.3.419

McGaugh, J. L. (2000). Memory—A Century of Consolidation. *Science*, *287*(5451), 248–251. https://doi.org/10.1126/science.287.5451.248

Mitra, A., Snyder, A. Z., Hacker, C. D., Pahwa, M., Tagliazucchi, E., Laufs, H., Leuthardt, E. C., & Raichle, M. E. (2016). Human cortical–hippocampal dialogue in wake and slow-wave sleep. *Proceedings of the National Academy of Sciences*, *113*(44), E6868–E6876. https://doi.org/10.1073/pnas.1607289113

Ngo, H.-V., Fell, J., & Staresina, B. (2020). Sleep spindles mediate hippocampal-neocortical coupling during long-duration ripples. *ELife*, *9*, e57011. https://doi.org/10.7554/eLife.57011

Ngo, H.-V., & Staresina, B. (2022). Shaping overnight consolidation via slow-oscillation closed-loop targeted memory reactivation. *Proceedings of the National Academy of Sciences*, *119*(44), e2123428119. https://doi.org/10.1073/pnas.2123428119

Nir, Y., Vyazovskiy, V. V., Cirelli, C., Banks, M. I., & Tononi, G. (2015). Auditory Responses and Stimulus-Specific Adaptation in Rat Auditory Cortex are Preserved Across NREM and REM Sleep. *Cerebral Cortex*, *25*(5), 1362–1378. https://doi.org/10.1093/cercor/bht328

Oostenveld, R., Fries, P., Maris, E., & Schoffelen, J.-M. (2011). FieldTrip: Open Source Software for Advanced Analysis of MEG, EEG, and Invasive Electrophysiological Data. *Computational Intelligence and Neuroscience*, *2011*, 1–9. https://doi.org/10.1155/2011/156869

Paller, K. A., & Wagner, A. D. (2002). Observing the transformation of experience into memory. *Trends in Cognitive Sciences*, *6*(2), 93–102. https://doi.org/10.1016/S1364-6613(00)01845-3

Perrin, F., García-Larrea, L., Mauguière, F., & Bastuji, H. (1999). A differential brain response to the subject's own name persists during sleep. *Clinical Neurophysiology*, *110*(12), 2153–2164. https://doi.org/10.1016/S1388-2457(99)00177-7

Rasch, B., Büchel, C., Gais, S., & Born, J. (2007). Odor Cues During Slow-Wave Sleep Prompt Declarative Memory Consolidation. *Science*, *315*(5817), 1426–1429. https://doi.org/10.1126/science.1138581

Roediger, H. L., & Butler, A. C. (2011). The critical role of retrieval practice in long-term retention. *Trends in Cognitive Sciences*, *15*(1), 20–27. https://doi.org/10.1016/j.tics.2010.09.003

Rolls, E. (2013). The mechanisms for pattern completion and pattern separation in the hippocampus. *Frontiers in Systems Neuroscience*, *7*. https://www.frontiersin.org/articles/10.3389/fnsys.2013.00074

Rothschild, G., Eban, E., & Frank, L. M. (2017). A cortical–hippocampal–cortical loop of information processing during memory consolidation. *Nature Neuroscience*, *20*(2), Article 2. https://doi.org/10.1038/nn.4457

Rudoy, J. D., Voss, J. L., Westerberg, C. E., & Paller, K. A. (2009). Strengthening Individual Memories by Reactivating Them During Sleep. *Science*, *326*(5956), 1079–1079. https://doi.org/10.1126/science.1179013

Schapiro, A. C., McDevitt, E. A., Rogers, T. T., Mednick, S. C., & Norman, K. A. (2018). Human hippocampal replay during rest prioritizes weakly learned information and predicts memory performance. *Nature Communications*, *9*(1), Article 1. https://doi.org/10.1038/s41467-018-06213-1

Schönauer, M. (2018). Sleep Spindles: Timed for Memory Consolidation. *Current Biology*, *28*(11), R656–R658. https://doi.org/10.1016/j.cub.2018.03.046

Schönauer, M., Alizadeh, S., Jamalabadi, H., Abraham, A., Pawlizki, A., & Gais, S. (2017). Decoding material-specific memory reprocessing during sleep in humans. *Nature Communications*, *8*(1), Article 1. https://doi.org/10.1038/ncomms15404

Schreiner, T., Doeller, C. F., Jensen, O., Rasch, B., & Staudigl, T. (2018). Theta Phase-Coordinated Memory Reactivation Reoccurs in a Slow-Oscillatory Rhythm during NREM Sleep. *Cell Reports*, *25*(2), 296–301. https://doi.org/10.1016/j.celrep.2018.09.037

Schreiner, T., Lehmann, M., & Rasch, B. (2015). Auditory feedback blocks memory benefits of cueing during sleep. *Nature Communications*, *6*(1), Article 1. https://doi.org/10.1038/ncomms9729

Schreiner, T., Petzka, M., Staudigl, T., & Staresina, B. P. (2021). Endogenous memory reactivation during sleep in humans is clocked by slow oscillation-spindle complexes. *Nature Communications*, *12*(1), Article 1. https://doi.org/10.1038/s41467-021-23520-2

Shanahan, L. K., Gjorgieva, E., Paller, K. A., Kahnt, T., & Gottfried, J. A. (2018). Odor-evoked category reactivation in human ventromedial prefrontal cortex during sleep promotes memory consolidation. *ELife*, *7*, e39681. https://doi.org/10.7554/eLife.39681

Squire, L. R. (1992). Memory and the hippocampus: A synthesis from findings with rats, monkeys, and humans. *Psychological Review*, *99*, 195–231. https://doi.org/10.1037/0033-295X.99.2.195

Staresina, B. P., & Wimber, M. (2019). A Neural Chronometry of Memory Recall. *Trends in Cognitive Sciences*, *23*(12), 1071–1085. https://doi.org/10.1016/j.tics.2019.09.011

Sterpenich, V., van Schie, M. K. M., Catsiyannis, M., Ramyead, A., Perrig, S., Yang, H.-D., Van De Ville, D., & Schwartz, S. (2021). Reward biases spontaneous neural reactivation during sleep. *Nature Communications*, *12*(1), Article 1. https://doi.org/10.1038/s41467-021-24357-5

Wang, B., Antony, J. W., Lurie, S., Brooks, P. P., Paller, K. A., & Norman, K. A. (2019). Targeted Memory Reactivation during Sleep Elicits Neural Signals Related to Learning Content. *Journal of Neuroscience*, *39*(34), 6728–6736. https://doi.org/10.1523/JNEUROSCI.2798-18.2019

Wei, Y., Krishnan, G. P., & Bazhenov, M. (2016). Synaptic Mechanisms of Memory Consolidation during Sleep Slow Oscillations. *The Journal of Neuroscience*, *36*(15), 4231–4247. https://doi.org/10.1523/JNEUROSCI.3648-15.2016

Wilson, M. A., & McNaughton, B. L. (1994). Reactivation of Hippocampal Ensemble Memories During Sleep. *Science*, *265*(5172), 676–679. https://doi.org/10.1126/science.8036517

Wislowska, M., Klimesch, W., Jensen, O., Blume, C., & Schabus, M. (2022). Sleep-Specific Processing of Auditory Stimuli Is Reflected by Alpha and Sigma Oscillations. *Journal of Neuroscience*, *42*(23), 4711–4724. https://doi.org/10.1523/JNEUROSCI.1889-21.2022

Xia, T., Yao, Z., Guo, X., Liu, J., Chen, D., Liu, Q., Paller, K. A., & Hu, X. (2022). Updating memories of unwanted emotions during human sleep. *Current Biology*. https://doi.org/10.1016/j.cub.2022.12.004

Yu, C., & Yao, W. (2017). Robust linear regression: A review and comparison. *Communications in Statistics - Simulation and Computation*, *46*(8), 6261–6282. https://doi.org/10.1080/03610918.2016.1202271

Zhang, H., Fell, J., & Axmacher, N. (2018). Electrophysiological mechanisms of human memory consolidation. *Nature Communications*, *9*(1), Article 1. https://doi.org/10.1038/s41467-018-06553-y

Züst, M. A., Ruch, S., Wiest, R., & Henke, K. (2019). Implicit Vocabulary Learning during Sleep Is Bound to Slow-Wave Peaks. *Current Biology*, *29*(4), 541-553.e7. https://doi.org/10.1016/j.cub.2018.12.038